Science of the Total Environment 633 (2018) 1602–1612

Contents lists available at ScienceDirect

Science of the Total Environment

journal homepage: www.elsevier.com/locate/scitotenv

Assessing the effect of chlorinated hydrocarbon degradation in aquitards on plume persistence due to back-diffusion

Philipp Wanner [a,*], Beth L. Parker [a], Daniel Hunkeler [b]

[a] G360 Institute for Groundwater Research, College of Engineering and Physical Sciences, University of Guelph, 50 Stone Road East, Guelph N1G 2W1, Ontario, Canada
[b] Centre for Hydrogeology & Geothermics (CHYN), University of Neuchâtel, Rue Emil Argand 11, CH-2000 Neuchâtel, Switzerland

HIGHLIGHTS

- Investigation of impact of reactive processes in aquitards on plume persistence.
- Development of 2D-numerical model of contaminated aquifer – aquitard system.
- Degradation activities in aquitards shorten plume persistence of parent compounds.
- Degradation in aquitard lead to unique $\delta^{13}C$ patterns in adjacent aquifer.
- Aquitard degradation can be inferred from $\delta^{13}C$ measurements in adjacent aquifer.

GRAPHICAL ABSTRACT

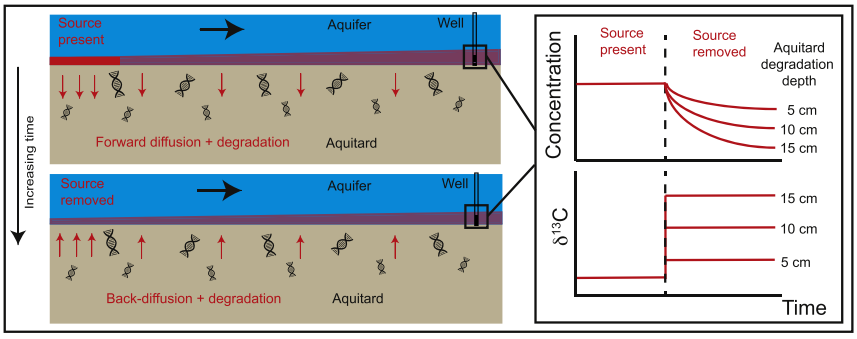

ARTICLE INFO

Article history:
Received 24 December 2017
Received in revised form 17 March 2018
Accepted 17 March 2018
Available online 5 April 2018

Editor: Frederic Coulon

Keywords:
Aquifer-aquitard system
Chlorinated hydrocarbons
Plume persistence
Back-diffusion
Degradation
Stable carbon isotopes

ABSTRACT

This modeling study aims to investigate how reactive processes in aquitards impact plume persistence in adjacent aquifers. For that purpose the migration of a trichloroethene (TCE) plume in an aquifer originating from dense non-aqueous phase liquid (DNAPL) source dissolution and back-diffusion from an underlying reactive aquitard was simulated in a 2D-numerical model. Two aquitard degradation scenarios were modeled considering one-step degradation from TCE to cis-dichloroethene (cDCE): a uniform (constant degradation with aquitard depth) and a non-uniform scenario (decreasing degradation with aquitard depth) and were compared with a no-degradation scenario. In the no-degradation scenario, a long-term TCE tailing above the Maximum Contaminant Level (MCL) caused by back-diffusion after source removal was observed. In contrast, in the aquitard degradation scenarios, TCE back-diffusion periods were shorter, whereby the extent of back-diffusion reduction depended on the aquitard degradation depth and the rate. For high degradation rates (half-life: 30–80 days), an aquitard degradation depth greater than 65 cm prevented TCE plume persistence after source removal but generated a long-term tailing above the MCL for the produced cDCE. For slow degradation rates (half-life: <200 days), TCE was only partially degraded after source removal, independent of the aquitard degradation depth, leading to a long-term dual contamination of the aquifer by cDCE and TCE. A sudden enrichment of ^{13}C in TCE and cDCE was observed after source removal in the uniform and non-uniform degradation scenarios that was distinct from $\delta^{13}C$ patterns observed when aquifer degradation occurs (continuous enrichment of ^{13}C along the plume axis) and for when there is absence of degradation (no change of isotope ratios). This demonstrates that $\delta^{13}C$ measurements in the aquifer can be used as a diagnostic tool to demonstrate aquitard degradation, which simplifies the identification of reactive processes in aquitards, as aquifers are usually easier to monitor than aquitards.

* Corresponding author at: G360 Institute for Groundwater Research, College of Engineering and Physical Sciences, University of Guelph, 50 Stone Road East, Guelph N1G 2W1, Ontario, Canada.
E-mail address: philipp.wanner@g360group.org. (P. Wanner).

https://doi.org/10.1016/j.scitotenv.2018.03.192
0048-9697/

1. Introduction

Subsurface contamination by chlorinated hydrocarbons is a widespread environmental problem (Pankow and Cherry, 1996). Chlorinated hydrocarbons are often released as dense non-aqueous phase liquids (DNAPLs) and rapidly migrate into the subsurface due to their high density, low viscosity and low interfacial tension (Pankow and Cherry, 1996; Schwille, 1988). When large quantities are released, DNAPLs migrate through the unsaturated zone and penetrate deep into aquifer systems. During migration in the saturated zone, DNAPLs form pools on top of low permeability layers, which dissolve slowly (Mackay and Cherry, 1989; Pankow and Cherry, 1996; Parker et al., 1994). The dissolved DNAPL compounds are then transported by advection in the aquifer creating a contaminant plume downgradient of the source and diffuse into the underlying low permeability units. Initially, it has been assumed that only the slow dissolution process of accumulated DNAPL pools on top of low permeability layers contributes to the longevity of DNAPL contamination sources (Anderson et al., 1992; Berglund, 1997; Hunt et al., 1988; Johnson and Pankow, 1992; Pankow and Cherry, 1996). However, in the early to mid-2000s, field and modeling studies showed that chlorinated hydrocarbon plumes can persist long after complete dissolution of accumulated DNAPL pools due to back-diffusion from aquitards (Chapman and Parker, 2005; Liu and Ball, 2002; Parker et al., 2008; Seyedabbasi et al., 2012). Using numerical modeling, it was demonstrated that back-diffusion can generate aquifer concentrations far above Maximum drinking water Concentration Limits (MCL, based on US EPA) for decades or even centuries (Chapman and Parker, 2005; Hwang et al., 2008; Seyedabbasi et al., 2012; Yang et al., 2017). These studies neglected reactive processes in the aquitard. However, the more reducing conditions in aquitards may frequently trigger degradation of chlorinated hydrocarbons, which are otherwise stable in oxic aquifers. Recent studies (Damgaard et al., 2013; Takeuchi et al., 2011; Wanner et al., 2016) confirmed that chlorinated hydrocarbons can indeed be degraded in aquitards. Hence, an investigation of the effect of degradation in aquitards on plume persistence is warranted. On the one hand, degradation could reduce plume longevity. On the other hand, if only partial degradation occurs, toxic transformation products might be released into the aquifer. The limited knowledge about degradation in aquitards is partly due to the difficulty in sampling water from this zone and the lack of suitable tools to demonstrate degradation. Compound-specific isotope analysis (CSIA) is a potential tool to demonstrate degradation in aquitards. However, it remains unclear how reactive processes in aquitards are reflected in isotope ratio patterns in aquifer – aquitard systems and whether stable isotope methods provide unequivocal insight into the relation between degradation activities in aquitards and plume persistence due to back-diffusion.

To address these research gaps, we investigate how reactive processes in aquitards influence plume persistence in adjacent aquifers using a 2D-numerical model. We evaluate to what extent aquitard degradation shortens the back-diffusion period of the parent compound for different degradation rates and aquitard degradation depths. We also consider the common scenario of only partial degradation and explore under what conditions elevated concentrations of daughter products can be expected in the overlying aquifer. Finally, as degradation in aquitards is more difficult to substantiate, we also investigate if aquitard degradation can be inferred from CSIA in aquifer samples.

2. Numerical simulation methods

2.1. Concept and set up of 2D-numerical simulations

The 2D-numerical model simulates the migration of a TCE plume in an aquifer. The plume originates from DNAPL source dissolution and back-diffusion from the underlying aquitard after source removal. This configuration was chosen as it represents a common scenario at many contaminated sites (Ball et al., 1997; Chapman and Parker, 2005; DiFilippo and Brusseau, 2008; Liu and Ball, 2002; Parker et al., 2008). The 2D-simulation approach relies on the assumption that transverse horizontal dispersion in the simulated aquifer does not affect the concentration evolution in the center of the contaminant plume. The dimensions of the modeling domain and the physical properties of the aquifer – aquitard system were adopted from Chapman and Parker (2005) (Table 1). The 2D-numerical modeling domain was 15 m high and 300 m long, whereby the aquifer was 5 m and the aquitard 10 m thick (Fig. 1). In the modeling domain, a highly resolved rectangular mesh was generated with 94,200 rectangular elements. The mesh was especially refined at the aquifer – aquitard interface, where the rectangular elements were 20 times smaller than in the rest of the modeling domain. Simulations with a four times finer mesh (376,800 elements) did not change contaminant profile shapes (Fig. S1, Supporting Information (SI)) indicating that the mesh is sufficiently fine to minimize numerical dispersion. A linear groundwater flow velocity of 0.5 m/d was specified in the aquifer, while in the underlying aquitard the velocity was set to zero (Table 1). A trichloroethene (TCE) DNAPL line source of 0.1 m height was emplaced at the up-gradient end of the modeling domain at the bottom of the aquifer. The source was emplaced for 42 years and after its removal clean water flushed through the aquifer for 100 years causing back-diffusion from the aquitard towards the aquifer (Fig. 1). For simulating degradation in the aquitard, a one-step degradation process from TCE to cis-dichloroethene (cDCE) was considered, which has the advantage that the effect of a degrading parent (TCE) and an accumulating daughter compound (cDCE) can be evaluated. Furthermore, the accumulation of cDCE, represents a common scenario at many sites, as sequential reductive dechlorination of chlorinated ethenes often stalls at cDCE (Aelion et al., 2010). To assess the impact of different aquitard degradation conditions on plume persistence and to investigate if they can be tracked by carbon isotope ratios, two different aquitard degradation scenarios were simulated and compared with a no-degradation scenario: A non-uniform and a uniform degradation scenario (Fig. 1). In the non-uniform degradation scenario, the degradation rate constant decreased with increasing aquitard depth as observed by Wanner et al. (2016) at the Borden site in Ontario, Canada. This can be related to diffusing nutrients from the aquifer into the aquitard favoring stronger degradation close the aquifer – aquitard interface compared to greater depths (Wanner et al., 2016). The uniform degradation scenario was simulated for a constant vertical degradation rate, whereby the used degradation rate constant (half-life: 30 days) corresponded to the detected constant at the aquifer – aquitard interface at the Borden site (Wanner et al., 2016). Concentration and carbon isotope ratio profiles were evaluated 25 and 280 m downgradient from the source zone. The temporal concentration and carbon isotope ratio evolutions were assessed in hypothetical wells with a 1.5 m screened interval at the base of the aquifer to cover the main part of the contaminant plume also located at 25 and 280 m downgradient from the source.

To examine whether degradation in the aquifer and aquitard, respectively can be differentiated based on CSIA of chlorinated hydrocarbons in groundwater, an aquifer-only degradation scenario was simulated and compared with the aquitard degradation scenarios (uniform and non-uniform). For the aquifer-only degradation scenario, a degradation rate constant of 4.72E-9 1/s (half-life = 170 days) was imposed, which is in the range of frequently detected degradation rate constants in aquifers (Wiedemeier et al., 1999). To compare carbon isotope ratios for the aquifer-only and the aquitard degradation scenarios, the spatial carbon isotope ratio evolution along the plume axis was assessed before source removal and for 100 years thereafter.

2.2. Governing equations

The 2D-reactive transport of TCE in the aquifer – aquitard system was simulated by using the advection-dispersion-reaction equation

Table 1
Model parameters for simulating the TCE plume in the aquifer – aquitard system.

Parameter	Unit	Value	Reference
Tortuosity factor	–	0.40	(Chapman and Parker, 2005)
K_{OC} TCE	L/Kg	126	(Chapman and Parker, 2005)
K_{OC} cDCE	L/Kg	86	(Chapman and Parker, 2005)
Diffusion coefficient in free solution: $D_{0,TCE}$	m^2/s	1.01E-09	(Chapman and Parker, 2005)
Diffusion coefficient in free solution: $D_{0,cDCE}$	m^2/s	1.13E-09	(Chapman and Parker, 2005)
Aquifer			
Height	m	5	(Chapman and Parker, 2005)
Length	m	300	(Chapman and Parker, 2005)
Hydraulic conductivity: K	m/s	2.0E-04	(Chapman and Parker, 2005)
Porosity: ϕ	–	0.35	(Chapman and Parker, 2005)
Linear groundwater flow velocity:v	m/d	0.5	(Chapman and Parker, 2005)
Organic carbon content: f_{OC}	%	0.038	(Chapman and Parker, 2005)
Bulk density: ρ	g/cm^3	1.70	(Chapman and Parker, 2005)
Transverse dispersivity: α_T	m	1.0	(Chapman and Parker, 2005)
Vertical dispersitvity: α_L	m	0.002	(Chapman and Parker, 2005)
Degradation rate constant k	1/s	4.7E-8	(Wiedemeier et al., 1999)
Isotopic enrichment factor degradation	‰	−18.2	(Wanner et al., 2016)
Isotopic enrichment factor sorption	‰	−0.40	(Wanner et al., 2017)
Isotopic enrichment factor diffusion	‰	−0.33	(Wanner and Hunkeler, 2015)
Aquitard			
Height	m	10	(Chapman and Parker, 2005)
Length	m	300	(Chapman and Parker, 2005)
Hydraulic conductivity: K	m/s	5.0E-10	(Chapman and Parker, 2005)
Porosity: ϕ	–	0.43	(Chapman and Parker, 2005)
Organic carbon content: f_{OC}	%	0.054	(Chapman and Parker, 2005)
Bulk density: ρ	g/cm^3	1.95	(Chapman and Parker, 2005)
Uniform degradation rate constant k	1/s	2.7E-7	(Wanner et al., 2016)
Non-uniform degradation rate constant k	1/s	$k_{init}\cdot erfc(az)$[a]	(Wanner et al., 2016)
Isotopic enrichment factor degradation	‰	−18.2	(Wanner et al., 2016)
Isotopic enrichment factor sorption	‰	−0.40	(Wanner et al., 2017)
Isotopic enrichment factor diffusion	‰	−0.33	(Wanner and Hunkeler, 2015)
TCE line source			
Height	m	0.1	(Chapman and Parker, 2005)
Concentration	mg/L	1100	(Chapman and Parker, 2005)
Persistence time	y	42	(Chapman and Parker, 2005)
$\delta^{13}C$	‰	−29.3	(Aelion et al., 2010)

[a] z corresponds to the vertical depth, k_{init} is the aquifer –aquitard degradation rate constant and a determines the degradation depth. k_{init} was varied in a range between 2.70E-7 and 2.01E-8 1/s (half-life: 30–400 days), while a was varied between 0.2 and 30.

for porous saturated media:

$$R_n\frac{\partial(\phi C_n)}{\partial t} = D_L\frac{\partial C_n}{\partial x^2} + D_T\frac{\partial C_n}{\partial z^2} - v\frac{\partial C_n}{\partial x} + r \quad (1)$$

where x (m) is the horizontal distance, z (m) the vertical depth, C_n (mmol/L) the concentration of species n, v (cm/y) the linear flow velocity in x direction, D_L (m^2/s) the longitudinal dispersion coefficient, D_T (m^2/s) the transversal dispersion coefficient and R_n (−) the retardation factor, ϕ (−) the porosity, and r (mmol/L·s) is the degradation rate. The advection-dispersion-reaction equation was solved numerically with the finite element computer code Comsol Multiphysics® using an implicit time-dependent solver algorithm and the BDF (backward differentiation formulas) time stepping method.

The transverse and longitudinal dispersion coefficients (Eq. (1)) are determined by using the following relationships:

$$D_T = D_e + \alpha_T v \quad (2)$$

$$D_L = D_e + \alpha_L v \quad (3)$$

where D_T and D_L (m^2/s) are the transverse and longitudinal dispersion coefficient, respectively, D_e (m^2/s) is the effective diffusion coefficient, α_T and α_L (m) refer to the transverse and longitudinal dispersivity, respectively and v (m/s) is the linear flow velocity in x direction. In the aquitard, the advective velocity was set to zero and hence, the dispersion coefficient reduces to the effective diffusion coefficient.

The effective diffusion coefficient (Eqs. (2) and (3)) includes the reduction of the diffusive transport rate in porous media due porosity and tortuosity effects and is defined as follows:

$$D_e = D_0\phi\tau \quad (4)$$

where D_0 (m^2/s) is the diffusion coefficient in free solution and τ (−) refers to the tortuosity factor.

The retardation factor (Eq. (1)) is defined assuming linear equilibrium sorption as:

$$R = 1 + \left(\frac{\rho_b}{\phi}\right)\cdot K_d \quad (5)$$

where ρ_b (g/cm^3) is the dry soil bulk density and K_d (L/kg) is the sorption equilibrium partition coefficient. The K_d values were estimated using the relationship $K_d = K_{OC}\cdot f_{OC}$, where K_{OC} is the porous medium organic carbon-water partition coefficient and f_{OC} is the solid phase organic carbon content.

The degradation of TCE to cDCE (r in Eq. (1)) was simulated in the 2D-numerical model using a first order degradation rate law:

$$r_{TCE} = -r_{cDCE} = -k\cdot C_{TCE} \quad (6)$$

where r (mmol/L·s) is the degradation rate, k (1/s) is the degradation rate constant and C_{TCE} (mmol/L) is the TCE concentration.

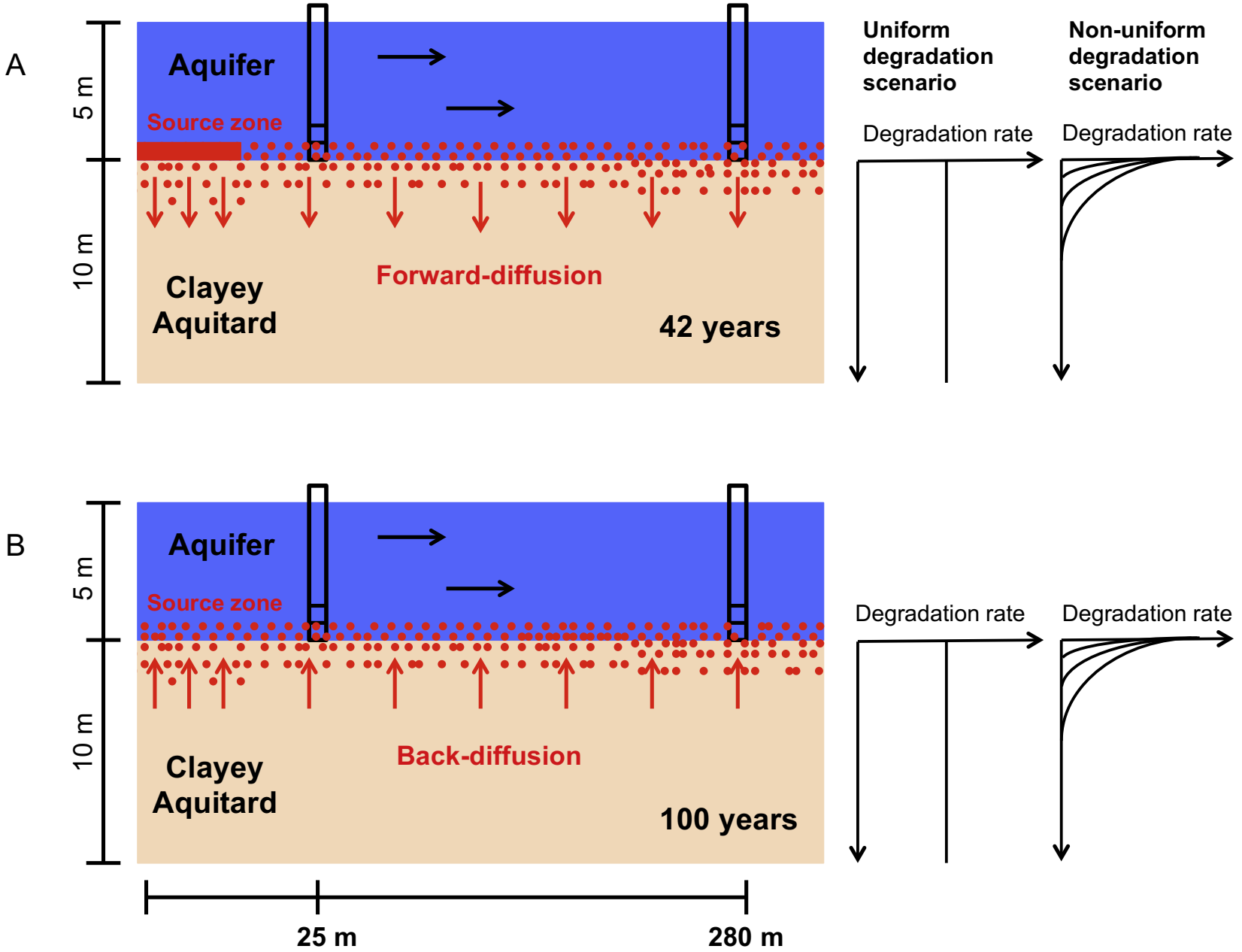

Fig. 1. Concept of 2D-numerical simulation of the contaminated aquifer – aquitard system modified after Chapman and Parker (2005). A TCE DNAPL source was emplaced for 42 years at the upgradient end of the modeling domain (A). Afterwards, the TCE DNAPL source was removed and the aquifer flushed with clean water for 100 years causing back-diffusion from the aquitard (B). A uniform and a non-uniform aquitard degradation scenario was simulated and compared with a no-degradation scenario. Concentration and carbon isotope profiles were evaluated 25 and 280 m downgradient from the source zone. The temporal concentration evolution was assessed in hypothetical wells with a 1.5 m screened interval at the base of the aquifer also located at 25 and 280 m downgradient from the source.

In the aquifer and in the uniform aquitard degradation scenario, a constant k value was used. In the non-uniform degradation scenario, k (Eq. (6)) followed an inverse error function with aquitard depth accounting for the decrease of the degradation rate with aquitard depth as observed by Wanner et al. (2016) at the Borden site:

$$k = k_{int} \cdot \ erfc(a \cdot z) \tag{7}$$

where k_{int} (1/s) is the aquifer – aquitard interface degradation rate constant, a (1/meters) is the parameter that defines how strongly the degradation rate constant decreases with depth and z is the vertical depth (meters).

The non-uniform degradation scenario was simulated for different aquifer – aquitard interface degradation rate constants (k_{int}, Eq. (7)) and for varying degradation depths. The degradation depth was defined as the depth at which the degradation rate constant has dropped to 8.03E-09 1/s (half-life: 1000 days) according to the inverse error function (Fig. S2. SI). The degradation rate constant at the aquifer – aquitard interface (k_{int}, Eq. (7)) was varied in a range between 2.70E-7 and 2.01E-8 1/s (half-lives: 30–400 days), whereas the aquitard degradation depth was changed between 0.051 and 2.97 m by varying the a-values between 0.2 and 30 in Eq. (7).

2.3. Isotope fractionation processes

In the 2D-numerical reactive transport model, carbon isotope fractionation caused by TCE transformation to cDCE and by physical processes (aqueous phase diffusion and sorption) were considered. For that purpose, species containing one heavy (^{13}C) and only light (^{12}C) carbon isotopes, respectively, were defined for TCE and cDCE (^{13}TCE, ^{12}TCE, ^{13}cDCE, ^{12}cDCE) in the model database. Molecules containing more than one heavy carbon isotope (^{13}C) were neglected, as the natural abundance of ^{13}C is low (1.1%) (Aelion et al., 2010). A $\delta^{13}C$ value of −29.3‰ was used for the TCE DNAPL source, which corresponds to an average value ($n = 10$) of different TCE manufacturers (Aelion et al., 2010). For simulating isotope fractionation associated with TCE degradation to cDCE, different degradation rate constants were assigned to isotopically distinct species according to van Breukelen et al. (2005) using an average ($n = 36$) isotope enrichment factor of $\varepsilon_{Degradation} = -18.2‰$ (Table 1) (Wanner et al., 2016):

$$^{12TCE}k = -^{12cDCE}k = -k \cdot f^{12}TCE \tag{8}$$

$$^{13TCE}k = -^{13cDCE}k = -k \cdot \left(\frac{\varepsilon_{Degradation}}{1000} + 1\right) \cdot f^{13}TCE \tag{9}$$

where $\varepsilon_{Degradation}$ is the degradation-induced isotope enrichment factor (Table 1) and f^{12}TCE, f^{13}TCE, f^{12}cDCE, f^{13}cDCE are the carbon isotopic species fractions of the total TCE and cDCE concentrations.

Isotopically light species sorb preferentially compared to heavy species (Kopinke et al., 2005; Wanner et al., 2017). To account for sorption-induced isotope fractionation, different K_d values (Eq. (5)) were assigned to each isotopic species based on the experimentally determined sorption-induced isotope enrichment factor of $\varepsilon_{Sorption} = -0.40‰$ (Table 1) by Wanner et al. (2017). Assuming that the K_d values for the more abundant species of TCE and cDCE (^{12}TCE and ^{12}cDCE) are equal to the K_d values of the total TCE and cDCE concentrations ($K_{d,TCE,total} \approx K_{d,12TCE}$ and $K_{d,cDCE,total} \approx K_{d,12cDCE}$) the K_d value for each individual isotopically distinct species is given by:

$$K_{d,^{12}TCE} = K_{d,TCE,total} \tag{10}$$

$$K_{d,^{13}TCE} = \left(\frac{\varepsilon_{sorption}}{1000} + 1\right) \cdot K_{d,TCE,total} \tag{11}$$

$$K_{d,^{12}cDCE} = K_{d,cDCE,total} \tag{12}$$

$$K_{d,^{13}cDCE} = \left(\frac{\varepsilon_{sorption}}{1000} + 1\right) \cdot K_{d,cDCE,total} \tag{13}$$

where $\varepsilon_{sorption}$ is the sorption-induced isotope enrichment factor, and K_d (L/kg) is the sorption equilibrium partition coefficient (Table 1).

The aqueous phase diffusive transport rate is slightly faster for light compared to isotopically heavy species (Wanner and Hunkeler, 2015). To include isotope fractionation due to aqueous phase diffusion, different diffusion coefficients D_0 (Eq. (3)) were defined for each of the simulated isotopically distinct species by using the experimentally determined diffusion-induced isotope enrichment factor of $\varepsilon_{Diffusion} = -0.33‰$ (Table 1) published by Wanner and Hunkeler (2015) (Table 1). It was assumed that the diffusion coefficients for the more abundant TCE and cDCE species (^{12}TCE and ^{12}cDCE) are equal to the diffusion coefficients of the total TCE and cDCE concentrations ($D_{0,TCE,total} \approx D_{0,12TCE}$ and $D_{0,cDCE,total} \approx D_{0,12cDCE}$) and hence, the diffusion coefficient for each individual isotopic species becomes:

$$D_{0,^{12}TCE} = D_{0,TCE,total} \tag{14}$$

$$D_{0,^{13}TCE} = \left(\frac{\varepsilon_{Diffusion}}{1000} + 1\right) \cdot D_{0,TCE,total} \tag{15}$$

$$D_{0,^{12}cDCE} = D_{0,cDCE,total} \tag{16}$$

$$D_{0,^{13}cDCE} = \left(\frac{\varepsilon_{Diffusion}}{1000} + 1\right) \cdot D_{0,cDCE,total} \tag{17}$$

where $\varepsilon_{Diffusion}$ is the diffusion-induced isotope enrichment factor and D (m^2/s) is the diffusion coefficient (Table 1).

3. Results and discussion

3.1. Vertical aquifer – aquitard concentration profiles

For all three scenarios (no-degradation, uniform and non-uniform degradation), the aquifer - aquitard concentration profiles are evaluated 280 m downgradient of the TCE DNAPL source. In addition, concentration profiles at 25 m distance from the source are presented in section 2 of the SI. In the no-degradation scenario, just before TCE DNAPL source removal at 42 years, the highest TCE concentration of 108 mg/L was observed at the aquifer – aquitard interface (Fig. 2A). In the aquitard, TCE showed distinct concentration profiles, whereby the concentration dropped below 0.1 mg/L at 4.5 m depth. Five years after source removal, the TCE concentration at the aquifer – aquitard interface had decreased to 6 mg/L, while in the aquitard typical back-diffusion profiles were observed showing the highest TCE concentration of 58 mg/L 0.65 m below the aquifer – aquitard interface (Fig. 2A). With increasing time (10–100 years after source removal), the TCE aquifer – aquitard interface concentrations further decreased and in the aquitard the peak concentrations of the back-diffusion profiles declined and migrated to greater depth.

For uniform degradation, the TCE concentration (53 mg/L) was half as high in the aquifer close to the aquifer - aquitard interface compared to the no-degradation scenario (108 mg/L) before source removal (Fig. 2B). Furthermore, the TCE concentrations in the aquitard were much lower and dropped below 0.1 mg/L at a shallower depth (0.23 m) than for the no-degradation scenario (4.5 m). Five years after source removal, TCE was no longer present neither in the aquifer nor in the aquitard (Fig. 2B). The same was observed closer to the source at 25 m distance (Fig. S3B, SI). Thus, the uniform degradation activities (half-life: 30 days) in the aquitard led to complete removal of TCE from the aquifer – aquitard systems five years after source removal. In contrast to the degraded TCE, the cDCE produced in the aquitard was observed in the aquifer and in the aquitard before and after source removal (Fig. 2C). In the aquitard, cDCE showed back-diffusion like

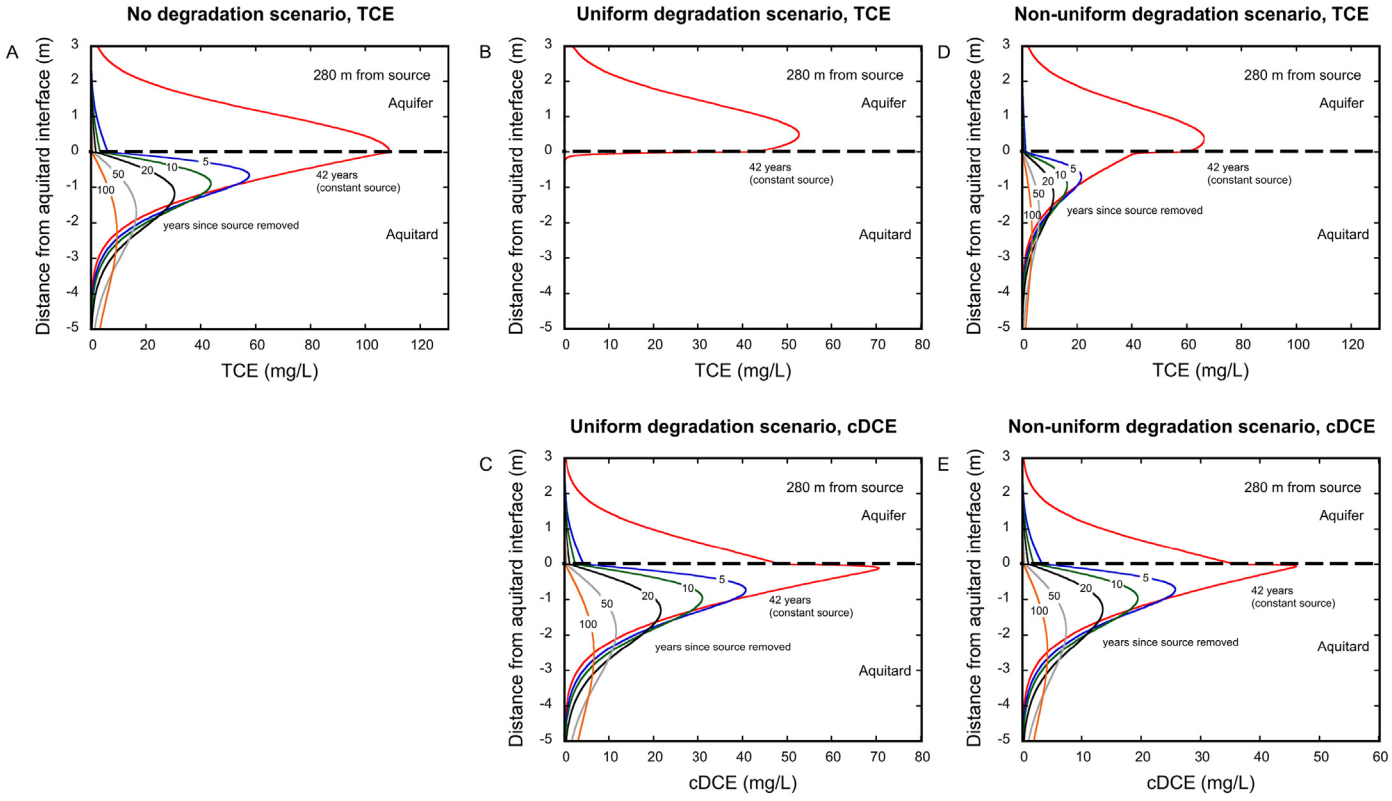

Fig. 2. Simulated TCE and cDCE concentration profiles 280 m down-gradient of the TCE DNAPL source for the no-degradation scenario (A), the uniform degradation scenario with a degradation rate constant of 2.70E-7 1/s (half-life: 30 days) (B and C) and the non-uniform degradation scenario with an aquifer – aquitard interface degradation rate constant of 2.70E-7 1/s (half-life: 30 days) and a degradation depth of 0.077 m (D and E). Concentration profiles are shown at the end of the 42 years constant source period and at 5, 10, 20, 50 and 100 years after source removal.

profiles with gradually decreasing concentrations with depth and towards the aquifer – aquitard interface. During the presence of the TCE DNAPL source, the peak concentration (70 mg/L) of the cDCE profile in the aquitard was observed next to the aquitard – aquifer interface. After source removal, the cDCE peak concentrations in the aquitard declined and moved downwards into the aquitard (Figs. 2C).

For the non-uniform degradation scenario, the concentration profiles are shown for a high aquifer – aquifer interface degradation rate constant of 2.7E-7 1/s (half-life: 30 days) and for an aquitard degradation depth of 0.077 m (Fig. 2D and E). These parameters correspond to the Borden site aquitard conditions observed by Wanner et al. (2016). Before source removal, the TCE aquifer concentration at the aquifer – aquitard interface (66 mg/L) was higher than in the uniform degradation scenario (53 mg/L), but lower than in the no-degradation scenario (108 mg/L, Fig. 2D). In the aquitard, the TCE concentration dropped below 0.1 mg/L at 4.15 m, which is deeper compared to the uniform degradation scenario (0.23 m) but shallower than in the no-degradation scenario (4.5 m). In contrast to the uniform degradation scenario, TCE was still present in the aquifer and in the aquitard up to 100 years after source removal (Fig. 2D and E), which was also observed closer to the source at 25 m distance (Fig. S3D–E, SI). In the aquitard, TCE showed distinct back-diffusion profiles with about three times lower concentrations than in the no-degradation scenario. The produced cDCE in the aquitard also showed back-diffusion like concentration patterns as in the uniform degradation scenario but at approximately 1.5 times lower concentrations (Fig. 2E).

3.2. Temporal concentration evolution in the aquifer

To evaluate the effect of the different aquitard degradation scenarios on plume persistence, breakthrough curves in a hypothetical 1.5 m screened well placed at the bottom of the aquifer 280 m downgradient of the source were assessed (Fig. 3A–B). Additionally, breakthrough curves in the well closer to the source (25 m) are presented in section 2 of the SI. For the no-degradation scenario, the TCE concentration in the simulated well remained on a constant level of 83 mg/L during the presence of the source. After source removal, the TCE concentration decreased rapidly by more than one order of magnitude (Fig. 3A). However, TCE showed a long-term tailing with TCE concentrations between 4.70 and 0.14 mg/L (Fig. 3A). Similarly, a long-term tailing was also observed closer to the source (25 m) but at slightly lower concentrations (1.40–0.14 mg/L, Fig. S4A, SI). Consequently, in the no-degradation scenario, the TCE concentrations in the aquifer remained several magnitudes above the MCL (0.005 mg/L, based on US EPA) for more than 100 years after source removal due to back-diffusion. These findings are consistent with previous modeling studies for non-reactive aquifer-aquitard systems, which also predicted TCE aquifer concentrations above the MCL for 100 years after source removal or depletion (Chapman and Parker, 2005; Seyedabbasi et al., 2012; Yang et al., 2017).

In the uniform degradation scenario, the TCE concentration in the simulated well remained on a lower level compared to the no-degradation scenario during the presence of the source (46 mg/L; Fig. 3A). The lower TCE concentrations are due to a stronger diffusive mass flux into the aquitard driven by the steeper aquifer - aquitard concentration gradient caused by aquitard degradation. After source removal, the TCE concentration in the well declined immediately below the MCL (Fig. 3A). The same was observed at 25 m distance from the source (Fig. S4A, SI). Hence, uniform degradation (half-life: 30 days) in the aquitard prevents a long-term tailing for TCE. This contrasts the no-degradation scenario, in which a long-term tailing for more than 100 years was observed (Fig. 3A). However, in the uniform degradation scenario, cDCE was produced in the aquitard and diffused towards the aquifer (Fig. 3B). During the presence of the source, the diffusive

transport of cDCE was largest resulting in a cDCE aquifer concentration of 27 mg/L (Fig. 3B). After the source was removed, the cDCE concentrations dropped but cDCE persisted above the MCL (0.07 mg/L, based on US EPA) (Fig. 3B). This shows that although the uniform degradation activities in the aquitard impeded a long-term tailing for TCE, in case of an incomplete degradation, aquifer contamination persists for several decades due to back-diffusion of the degradation product.

For non-uniform degradation, the temporal concentration evolution in the well are presented for a high aquifer – aquitard interface degradation rate constant of 2.7E-7 1/s (half-life: 30 days) and for six different degradation depths (0.051 m, 0.077 m, 0.103 m, 0.154 m, 0.307 m) (Fig. 3A–B). During the presence of the source, the TCE concentrations prevailed on intermediate levels (61–48 mg/L) for the different degradation depths compared to the no-degradation (83 mg/L) and uniform degradation scenario (46 mg/L) (Fig. 3A) and cDCE occurred as well. The same was observed at 25 m distance from the source (Fig. S4A, SI). The aquifer – aquitard concentration gradient and the associated diffusive mass flux into the aquitard is stronger than in the no-degradation but weaker than in the uniform degradation scenario during the presence of the TCE DNAPL source leading to the intermediate concentration level. The effect of non-uniform versus uniform degradation during the presence of a TCE source was also investigated by Chambon et al. (2010) but for fractured clay. They simulated decreasing and constant degradation in the low permeable matrix with increasing distance from fractures and predicted higher TCE concentration in the adjacent high permeable fracture for non-uniform compared to uniform degradation. Although on a smaller scale, this is consistent with the simulated uniform and non-uniform degradation scenario of the present study. After source removal, the groundwater TCE concentration varied for the different aquitard degradation depths. For a degradation depth of 0.051 m, TCE remained above the MCL for more than 100 years after source removal. For greater aquitard degradation depths, TCE persisted at lower concentrations and for shorter times. The largest aquitard degradation depth (0.307 m) led to a TCE concentration decrease below the MCL two years after source removal (Fig. 3A). In addition to TCE, cDCE was also detected in the simulated well. Hence, significant diffusive transport of the produced cDCE in aquitard towards the aquifer not only occurs for the uniform but also for the non-uniform degradation scenario. During the presence of the source, higher cDCE concentrations were observed for greater compared to shallower aquitard degradation depths. After source removal, the cDCE concentrations decreased by several orders of magnitude but persisted above the MCL for all aquitard degradation depths for more than 100 years (Fig. 3B). The concentrations at which cDCE persisted after source removal was similar for the different aquitard degradation depths (Fig. 3B). This shows that the concentration of the cDCE long-term tailing after source removal is less sensitive to the aquitard degradation depth compared to TCE.

A comparison of the uniform and non-uniform degradation scenario highlights that the aquitard degradation depth has a strong influence on the TCE plume persistence. In addition, it is expected that the TCE plume persistence is sensitive to the degradation rate. To investigate the influence of the aquitard degradation depth and rate on TCE plume persistence, the required degradation depth to prevent TCE aquifer contamination by back-diffusion was determined for various aquifer-aquitard interface degradation rate constants (k_{init}, Eq. (7)). A TCE concentration drop below 0.001 mg/L within 0.2 years after source removal was used as the criteria for complete TCE elimination. For the highest degradation rate constant (half-life: 30 days), an aquitard degradation depth of 0.36 m is required (Fig. 4). With a decreasing degradation rate constant, the required degradation depth increases first slowly to 0.65 m depth for a degradation rate constant of 1.00E-07 1/s (half-life: 80 days). When further decreasing the degradation rate constant, the required degradation depth increases strongly and for a degradation rate constant lower than 5.00E-08 1/s (half-life: 160 days), TCE degradation is no longer sufficient to prevent significant back-diffusion of TCE (Fig. 4).

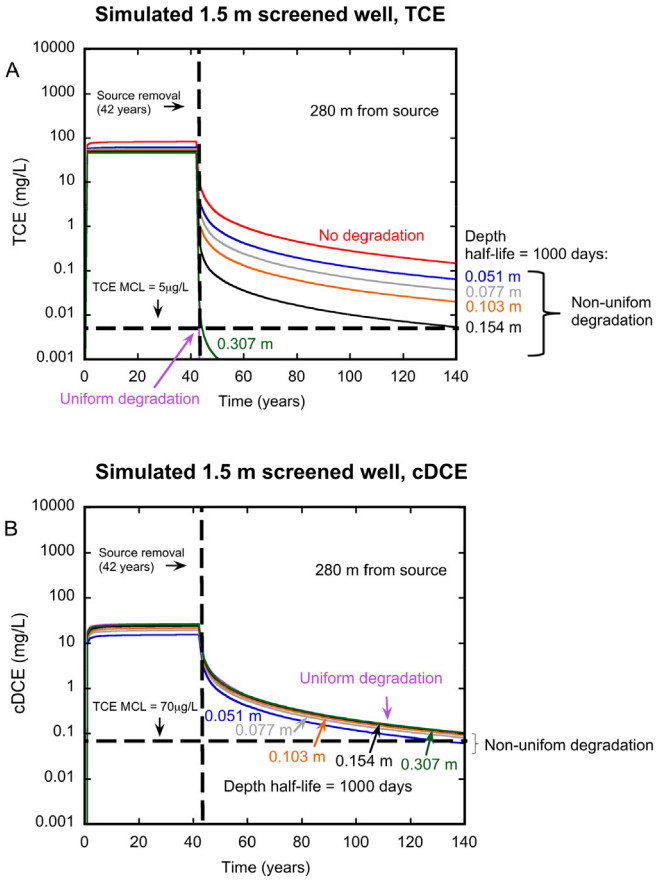

Fig. 3. Temporal TCE (A) and cDCE (B) concentration evolution in a hypothetical 1.5 m screened well, located 280 m downgradient of the TCE DNAPL source on top of the aquitard for the no-degradation, the uniform degradation scenario with a degradation rate constant of 2.70E-7 1/s (half-life: 30 days) and the non-uniform degradation scenario with an aquifer – aquitard interface degradation rate constant of 2.70E-7 1/s (half-life: 30 days) and degradation depths varying between 0.051 and 0.307 m. Maximum Contaminant Levels (MCL) for TCE (5 μg/L) and cDCE (70 μg/L) are indicated with the horizontal dashed lines based on the US EPA.

3.3. Vertical aquifer – aquitard carbon isotope ratio profiles

Similar to the concentration profiles, aquifer - aquitard TCE and cDCE carbon isotope ratio profiles are evaluated 280 m downgradient of the TCE DNAPL source for the three scenarios (no-degradation, uniform and non-uniform degradation). Supplementary, carbon isotope ratio profiles located closer to the source (25 m distance) are discussed in section 2 of the SI. The profiles were assessed to investigate how the different degradation conditions are reflected in carbon isotope ratio profiles and to investigate if the different degradation scenarios lead to unique isotope ratio patterns compared to a diffusion/back-diffusion scenario without degradation. In the no-degradation scenario, TCE carbon isotope ratios were temporally constant close to the aquifer – aquitard interface corresponding to the source signature ($\delta^{13}C = -29.3‰$). With increasing vertical distance below the aquifer–aquitard interface, the TCE became slightly depleted in ^{13}C in the aquitard (Fig. 5A). The small shifts can be explained by the faster diffusive transport rate for the isotopically light compared to the heavy species into the aquitard.

For the uniform degradation scenario, TCE was strongly enriched in ^{13}C in the top layer of the aquitard during the presence of the source due to the high degradation rate (half-life: 30 days) (Fig. 5B). The cDCE reached the initial carbon isotope signature of TCE at 0.20 m depth in the aquitard as TCE was completely converted to cDCE (Fig. 5C). With

increasing depth an inverse carbon isotope trend of cDCE was observed with a slight depletion of ^{13}C due to the diffusive transport process. After source removal, the inverse shift of the cDCE carbon isotope ratios with depth in the aquitard was less pronounced (Fig. 5C). This can be explained by the flatting of the concentration gradient after the source was removed, which lessens the diffusion-induced isotope effect (Wanner and Hunkeler, 2015). Furthermore, the cDCE carbon isotope profiles in the aquitard look similar as the TCE profiles in the no-degradation scenario after source removal. The cDCE acts as a contamination source for the adjacent aquifer similarly as TCE in the no-degradation scenario (Fig. 5C). In the aquifer, after source removal, cDCE became more enriched in ^{13}C reaching the isotope signature of the TCE. This trend can be explained by complete transformation of TCE to cDCE in the aquitard followed by diffusion towards the aquifer.

In the non-uniform degradation scenario, a pronounced enrichment of ^{13}C was observed in the upper 0.20 m of the aquitard during the presence of the source that is, however, less strong than in the uniform degradation scenario (Fig. 5D–E). With increasing depth an inverse trend with slight depletion of ^{13}C was detected caused by the diffusive transport. After source removal, TCE and cDCE carbon isotope ratios became more enriched in ^{13}C in the upper 0.20 m of the aquitard due to the ongoing degradation of the remaining TCE (Fig. 5D–E). The magnitude of the shift was largest in the aquitard adjacent to the aquifer – aquitard interface and decreased with depth due to vertically non-uniformly distributed degradation activities (Fig. 5D–E). At greater depth, TCE and cDCE were depleted in ^{13}C caused by the diffusive transport process as already observed during the presence of the source. Furthermore, the diffusion-induced isotope shift decreased with increasing time as the concentration gradient in the aquitard became flatter as observed in the uniform degradation scenario (Fig. 5D–E). In the aquifer, TCE and cDCE was more enriched in ^{13}C after source removal. This can be explained by the further degradation of TCE to cDCE during back-diffusion through the bioactive zone of the aquitard, leading to an enrichment of ^{13}C in the aquifer TCE and cDCE after source removal (Fig. 5D–E).

3.4. Temporal carbon isotope ratio evolution in aquifer

Analogously to the concentration breakthrough curves, the temporal carbon isotope ratio evolution of TCE and cDCE in the aquifer were evaluated 280 m downgradient of the source in a hypothetical 1.5 m screened well placed on top of the aquifer-aquitard interface. In addition, the temporal evolution of the carbon isotope signatures of TCE and cDCE closer to the source (25 m distance) is presented in section 2 of the SI. For the no-degradation scenario, the TCE carbon isotope ratios remained constant (Fig. 6A) indicating that physical isotope effects such as sorption and diffusion are not significantly modifying the TCE carbon isotope signature in the aquifer.

For the uniform degradation scenario, the TCE carbon isotope signature remained constant during the presence of the TCE DNAPL source but TCE was noticeably more enriched in ^{13}C ($\delta^{13}C = -24.3‰$) than in the no-degradation scenario ($\Delta\delta^{13}C = -29.3‰$) (Fig. 6A). Due to the more rapid degradation of light compared to heavy TCE in the aquitard, concentration gradients are steeper and thus, the diffusive mass flux into the aquitard is larger for light compared to heavy TCE, leading to the enrichment of ^{13}C in TCE in the aquifer. The cDCE carbon isotope signature was also constant ($\delta^{13}C = -35.4‰$) during the presence of the source (Fig. 6B). In contrast, after source removal, cDCE became immediately enriched in ^{13}C by 5‰, reaching the isotopic signature of the TCE source due to complete degradation of TCE to cDCE in the aquitard followed by back-diffusion towards the aquifer.

In the non-uniform degradation scenario similar $\delta^{13}C$ values were observed for TCE during the presence of the source for all simulated aquitards degradation depths. However, the $\delta^{13}C$ values were slightly more depleted than in the uniform degradation scenario (TCE: $\delta^{13}C = -24.8‰$). Due to the lower degree of TCE transformation in the non-uniform compared to the uniform degradation scenario concentration gradients are flatter and thus, the faster diffusive mass flux into the aquitard for the light compared to the heavy TCE is less pronounced leading to a weaker enrichment of ^{13}C in TCE in the aquifer. In contrast to TCE, the carbon isotope signatures of cDCE are more sensitive to the aquitard degradation depth during the presence of the source. For the shallowest degradation depth (0.051 m), cDCE showed a $\delta^{13}C$ value of −42.1‰, while cDCE becomes more enriched in ^{13}C for greater degradation depths, showing a $\delta^{13}C$ value of −37.2‰ for the largest degradation depth (0.307 m). A larger quantity of TCE is transformed to cDCE for deeper compared to shallower aquitard degradation depths leading to the observed stronger enrichment of ^{13}C in cDCE for deeper than for shallower degradation depths. After source removal, TCE and cDCE became suddenly enriched in ^{13}C. The same instant enrichment of ^{13}C in TCE and cDCE was also observed close to the source (25 m downgradient shown in Fig. S6A–B, SI). The immediate enrichment in ^{13}C after source removal was stronger for the deeper than for the shallower degradation depths. For a degradation depth of 0.051 m, an isotopic enrichment of 9.1‰ and 2.6‰ occurred for TCE and cDCE, respectively, while for a degradation depth of 0.307 m, the isotopic enrichment was 34.7‰ for TCE and 5.8‰ for cDCE, respectively. The sudden enrichment of TCE and cDCE in ^{13}C after source removal can be explained by the further degradation and enrichment in ^{13}C of the remaining TCE in the aquitard during its back-diffusive transport through the bioactive zone in the upper 0.051–0.307 m of the aquitard towards the aquifer (Fig. 6A). Furthermore, after source removal, carbon isotope signatures of TCE and cDCE in the aquifer remained constant despite transient temporal TCE and cDCE concentration evolutions (Fig. 6A–B) likely due to first order kinetic degradation approach, for which the magnitude of isotope fractionation shows no concentration dependency.

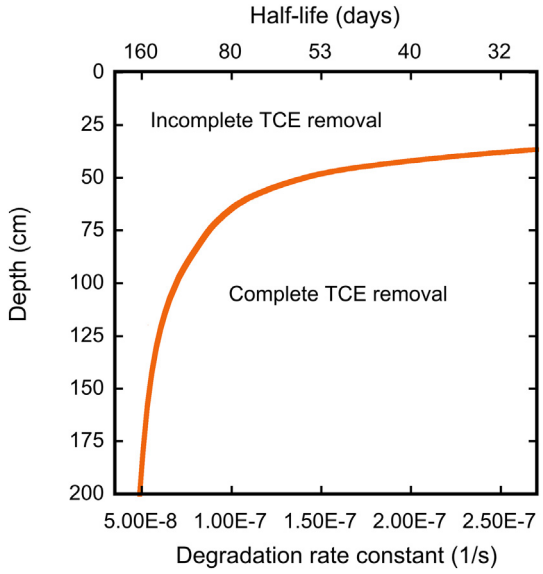

Fig. 4. Required aquitard degradation depth for completely eliminating TCE from the aquifer after source removal for varying aquifer – aquitard interface degradation rate constants (k_{init}, Eq. (7)).

3.5. Spatial carbon isotope signature evolution for degradation in the aquifer and for uniform and non-uniform degradation in the aquitard

To explore if carbon isotope ratio aquifer measurements can also be used to distinguish between reactive processes occurring in the aquifer

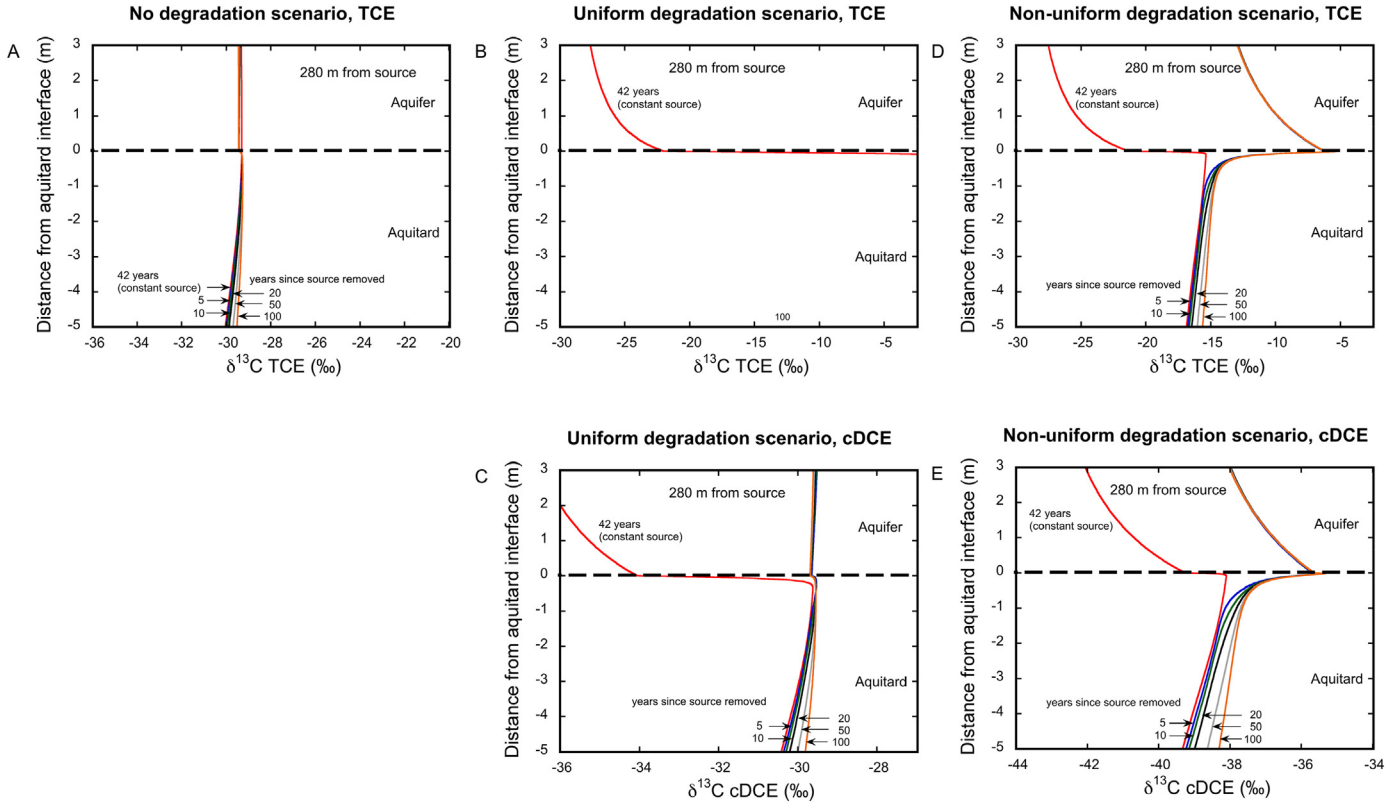

Fig. 5. Simulated TCE and cDCE carbon isotope ratio profiles 280 m down-gradient of the TCE DNAPL source for the no-degradation scenario (A), the uniform degradation scenario with degradation rate constant of 2.7E-7 1/s (half-life: 30 days) (B and C) and the non-uniform degradation scenario with an aquifer – aquitard interface degradation rate constant of 2.7E-7 1/s (half-life: 30 days) and a degradation depth of 0.077 m (D and E). Carbon isotope ratio profiles are shown at the end of the 42 years constant source period and at 5, 10, 20, 50 and 100 years after source removal.

or in the aquitard, the evolution of carbon isotope ratios along the plume axis was assessed in the aquifer-only and in the aquitard degradation scenarios (uniform and non-uniform). The non-uniform degradation scenario is shown for an aquifer – aquitard interface degradation rate constant of 2.70E-7 1/s (half-life: 30 days) and an aquitard degradation depth of 0.077 m. The spatial evolution of carbon isotope ratios along the plume axis was investigated just before and during 100 years after source removal. In the aquifer-only degradation scenario, a continuous enrichment of ^{13}C in TCE and cDCE was observed with increasing distance from the source (Fig. 7A and B). The enrichment of heavy cDCE and TCE carbon isotopes along the plume axis was similar before and during 100 years after the source was removed (Fig. 7A and B). This can be explained by the identical carbon isotope signature of TCE, which acts as contamination source before (TCE DNAPL) and after (back-diffusion of TCE from aquitard, mainly from source zone) source removal. In contrast, a smaller continuous enrichment of ^{13}C in TCE and cDCE along the plume axis was observed for the aquitard degradation scenarios (uniform and non-uniform) during the presence of the source. As only the small TCE portion that had diffused into the aquitard undergoes degradation and contributes to the enrichment of ^{13}C in the aquifer by back-diffusion, the enrichment of ^{13}C along the plume axis is smaller for the aquitard compared to the aquifer-only degradation scenario. Five years after source removal TCE and cDCE became enriched in ^{13}C in the aquitard degradation scenarios and remained equal for 100 years, due to the back-diffusive transport of TCE and cDCE through the bioactive aquitard zone (Fig. 7A–B). This is different from the similar enrichment of ^{13}C in TCE and cDCE before and after source removal in the aquifer-only degradation scenario. Therefore, the assessment of the spatial carbon isotope ratio evolution along the plume axis downgradient of the source before and after source removal is useful to identify whether organic contaminants are affected by degradation in the aquifer or in the aquitard. Furthermore, close to the source a distinction between aquifer and aquitard degradation is also possible based on the $\delta^{13}C$ values after source removal only. While for aquifer degradation the carbon isotope enrichment trend commences from the carbon isotope source signature, TCE and cDCE are already strongly enriched in ^{13}C close to the source zone in the aquitard degradation scenario as degradation occurs during the back-diffusion through the bioactive aquitard zone (Fig. 7A–B).

4. Conclusions

The results of the present modeling study demonstrate that the spatial variability of degradation activities in aquitards and the degradation rates have an impact on back-diffusion caused plume persistence in adjacent aquifers. For high aquitard degradation rates, an increase of the aquitard degradation depth by a few decimeters shortens the back-diffusion period of the parent compound by several decades. In contrast for low aquitard degradation rates, only partial degradation occurs and plume persistence of the parent compound cannot be avoided regardless of the aquitard degradation depth. Furthermore, one-step degradation from TCE to cDCE, can lead to elevated daughter compound concentrations in the adjacent aquifer due to its production in the aquitard followed by diffusive release to the adjacent aquifer. However, plume persistence of the daughter compounds are less sensitive to the aquitard degradation depth compared to the parent compounds. The rapid enrichment of ^{13}C in the aquifer after source removal is characteristic for aquitard degradation and clearly

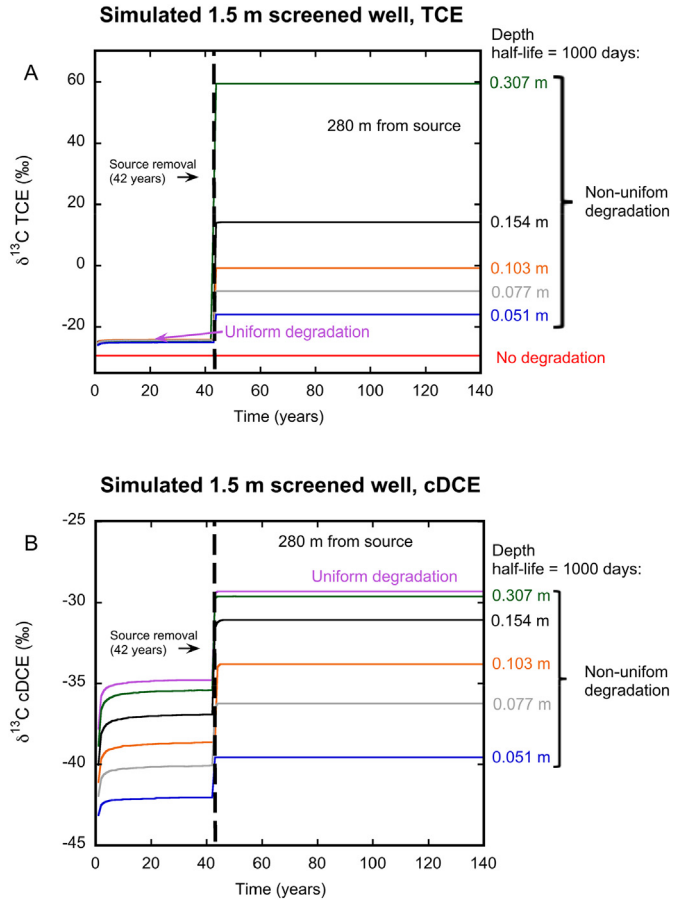

Fig. 6. Temporal carbon isotope ratio evolution of TCE (A) and cDCE (B) in a hypothetical 1.5 m screened well, located 280 m downgradient of the TCE DNAPL source on top of the aquitard for the no-degradation, the uniform degradation scenario with a degradation rate constant of 2.7E-7 1/s (half-life: 30 days) and the non-uniform degradation scenario with an aquifer – aquitard interface degradation rate constant of 2.7E-7 1/s (half-life: 30 days) and degradation depths varying between 0.051 and 0.307 m.

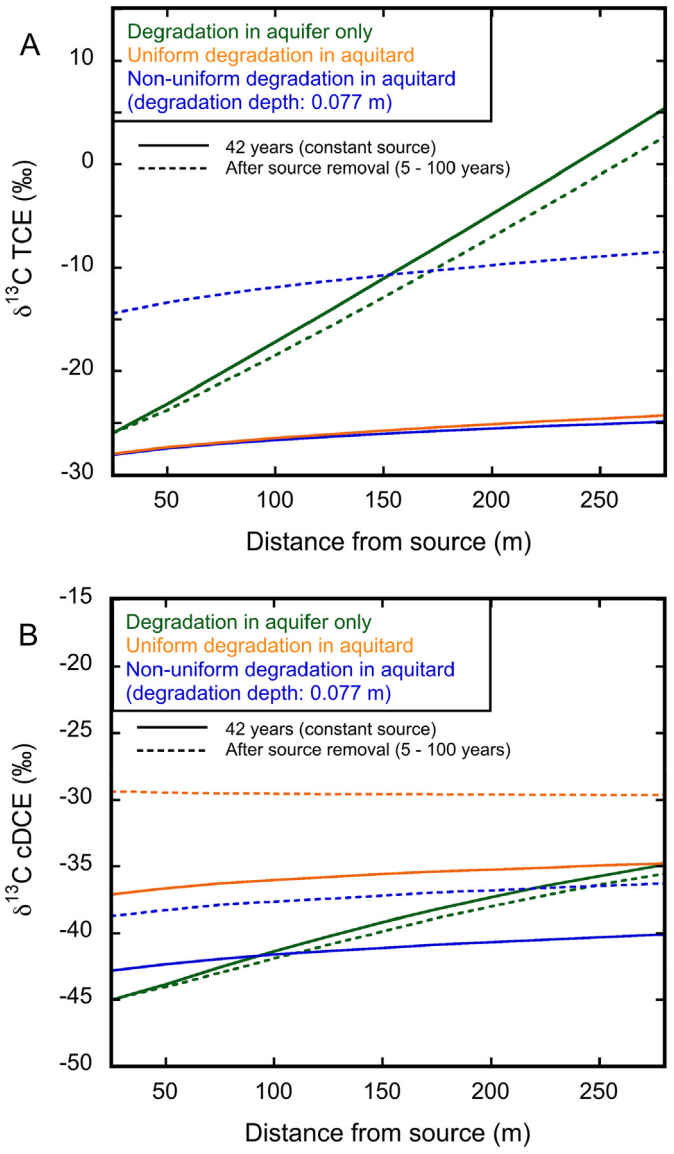

Fig. 7. Spatial carbon isotope ratio evolution along the plume axis for TCE (A) and cDCE (B) for the degradation scenario in the aquifer and for the uniform and the non-uniform aquitard degradation scenarios just before and 5–100 years after source removal. For the aquifer degradation scenario a degradation rate constant of 4.7E-8 1/s (half-life: 170 days) was imposed. For the uniform aquitard degradation scenario a degradation rate constant of 2.7E-7 1/s (half-life: 30 days) was used in the model, while for the non-uniform aquitard degradation scenario an aquifer – aquitard interface degradation rate constant of 2.7E-7 1/s (half-life: 30 days) and a degradation depth of 0.077 m was imposed in the simulations.

distinct from carbon isotope ratio patterns for aquifer degradation only (continuous enrichment of ^{13}C along the plume axis) or the no-degradation scenario (no change of isotope ratios). The characteristic carbon isotope ratio pattern for aquitard degradation demonstrates that CSIA in aquifer samples can be used as a diagnostic tool to demonstrate degradation in the aquitard. This greatly simplifies the identification of reactive processes in aquitards as aquifers are easier to access than aquitards through time by sampling monitoring wells. In addition, when degradation occurs in the aquitard the characteristic temporal carbon isotope ratio evolution in the aquifer is beneficial to reveal whether the remediation of a DNAPL source located in the aquifer was effective as the contaminants become enriched in ^{13}C when the DNAPL was completely removed. Hence, the gained insight from the present modeling study will generally facilitate improved site management decisions related to remedial actions for contaminated aquifer – aquitard systems.

Acknowledgement

The authors acknowledge the Swiss National Science Foundation (SNFS) (200021E-139877) for financial support.

Appendix A. Supplementary data

The simulations results at 25 m distance from the source are provided in the Supporting Information. Supplementary data to this article can be found online at https://doi.org/10.1016/j.scitotenv.2018.03.192.

References

Aelion, C., Hoehener, P., Hunkeler, D., Aravena, R., 2010. Environmental Isotopes in Biodegradation and Bioremediation. CRC Press, USA.

Anderson, M.R., Johnson, R.L., Pankow, J.F., 1992. Dissolution of dense chlorinated solvents into ground water: 1. Dissolution from a well-defined residual source. Ground Water 30, 250–256.

Ball, W.P., Liu, C.X., Xia, G.S., Young, D.F., 1997. A diffusion-based interpretation of tetrachloroethene and trichloroethene concentration profiles in a groundwater aquitard. Water Resour. Res. 33, 2741–2757.

Berglund, S., 1997. Aquifer remediation by pumping: a model for stochastic-advective transport with nonaqueous phase liquid dissolution. Water Resour. Res. 33, 649–661.

Chambon, J.C., Broholm, M.M., Binning, P.J., Bjerg, P.L., 2010. Modeling multi-component transport and enhanced anaerobic dechlorination processes in a single fracture-clay matrix system. J. Contam. Hydrol. 112, 77–90.

Chapman, S.W., Parker, B.L., 2005. Plume persistence due to aquitard back diffusion following dense nonaqueous phase liquid source removal or isolation. Water Resour. Res. 41.

Damgaard, I., Bjerg, P.L., Baelum, J., Scheutz, C., Hunkeler, D., Jacobsen, C.S., Tuxen, N., Broholm, M.M., 2013. Identification of chlorinated solvents degradation zones in

clay till by high resolution chemical, microbial and compound specific isotope analysis. J. Contam. Hydrol. 146, 37–50.
DiFilippo, E.L., Brusseau, M.L., 2008. Relationship between mass-flux reduction and source-zone mass removal: analysis of field data. J. Contam. Hydrol. 98, 22–35.
Hunt, J.R., Sitar, N., Udell, K.S., 1988. Nonaqueous phase liquid transport and cleanup: 1. Analysis of mechanisms. Water Resour. Res. 24, 1247–1258.
Hwang, Y.K., Endres, A.L., Piggott, S.D., Parker, B.L., 2008. Long-term ground penetrating radar monitoring of a small volume DNAPL release in a natural groundwater flow field. J. Contam. Hydrol. 97, 1–12.
Johnson, R.L., Pankow, J.F., 1992. Dissolution of dense chlorinated solvents into groundwater. 2. Source functions for pools of solvent. Environ. Sci. Technol. 26, 896–901.
Kopinke, F.D., Georgi, A., Voskamp, M., Richnow, H.H., 2005. Carbon isotope fractionation of organic contaminants due to retardation on humic substances: implications for natural attenuation studies in aquifers. Environ. Sci. Technol. 39, 6052–6062.
Liu, C.X., Ball, W.P., 2002. Back diffusion of chlorinated solvent contaminants from a natural aquitard to a remediated aquifer under well-controlled field conditions: predictions and measurements. Ground Water 40, 175–184.
Mackay, D.M., Cherry, J.A., 1989. Groundwater contamination - pump and treat remediation. 2. Environ. Sci. Technol. 23, 630–636.
Pankow, J.F., Cherry, J.A., 1996. Dense Chlorinated Solvents and Other DNAPLs in Groundwater. Waterloo Press, Portland, OR.
Parker, B.L., Gillham, R.W., Cherry, J.A., 1994. Diffusive disappearance of immiscible-phase organic liquids in fractured geologic media. Ground Water 32, 805–820.
Parker, B.L., Chapman, S.W., Guilbeault, M.A., 2008. Plume persistence caused by back diffusion from thin clay layers in a sand aquifer following TCE source-zone hydraulic isolation. J. Contam. Hydrol. 102, 86–104.
Schwille, F., 1988. Dense Chlorinated Solvents in Porous and Fractured Media: Model Experiments. Boca Raton, FL, USA.
Seyedabbasi, M.A., Newell, C.J., Adamson, D.T., Sale, T.C., 2012. Relative contribution of DNAPL dissolution and matrix diffusion to the long-term persistence of chlorinated solvent source zones. J. Contam. Hydrol. 134, 69–81.
Takeuchi, M., Kawabe, Y., Watanabe, E., Oiwa, T., Takahashi, M., Nanba, K., Kamagata, Y., Hanada, S., Ohko, Y., Komai, T., 2011. Comparative study of microbial dechlorination of chlorinated ethenes in an aquifer and a clayey aquitard. J. Contam. Hydrol. 124, 14–24.
van Breukelen, B.M., Hunkeler, D., Volkering, F., 2005. Quantification of sequential chlorinated ethene degradation by use of a reactive transport model incorporating isotope fractionation. Environ. Sci. Technol. 39, 4189–4197.
Wanner, P., Hunkeler, D., 2015. Carbon and chlorine isotopologue fractionation of chlorinated hydrocarbons during diffusion in water and low permeability sediments. Geochim. Cosmochim. Acta 157, 198–212.
Wanner, P., Parker, B., Chapman, S.W., Aravena, R., Hunkeler, D., 2016. Quantification of degradation of chlorinated hydrocarbons in saturated low permeability sediments using compound-specific isotope analysis (CSIA). Environ. Sci. Technol. 50 (11), 5622–5630.
Wanner, P., Parker, B.L., Chapman, S.W., Aravena, R., Hunkeler, D., 2017. Does sorption influence isotope ratios of chlorinated hydrocarbons under field conditions? Appl. Geochem. 84, 348–359.
Wiedemeier, T., Rifai, H., Newell, C., Wilson, J., 1999. Natural Attenuation of Fuels and Chlorinated Solvents in the Subsurface. John Wiley & Sons.
Yang, M., Annable, M.D., Jawitz, J.W., 2017. Field-scale forward and back diffusion through low-permeability zones. J. Contam. Hydrol. 202, 47–58.